REPORT DOCUMENTATION PAGE

AFRL-SR-AR-TR-04-

0259

1. AGENCY USE ONLY *(Leave blank)*	2. REPORT DATE	3. REPORT TYPE AND DATES COVERED
	20 APR 04	FINAL REPORT 1 JUN 01 - 30 NOV 03

4. TITLE AND SUBTITLE
NANOJETS: ELECTRIFICATION, ENERGETICS, DYNAMICS, STABILITY AND BREAKUP

5. FUNDING NUMBERS
F49620-01-1-0426
61102F
2305/TC

6. AUTHOR(S)
PROF UZI LANDMAN

7. PERFORMING ORGANIZATION NAME(S) AND ADDRESS(ES)
GEORGIA INSTITUTE OF TECHNOLOGY
SCHOOL OF PHYSICS
ATLANTA, GA 30332-0430

8. PERFORMING ORGANIZATION REPORT NUMBER

9. SPONSORING/MONITORING AGENCY NAME(S) AND ADDRESS(ES)
AFOSR/NL
4015 WILSON BLVD., SUITE 713
ARLINGTON, VA 22203-1954

10. SPONSORING/MONITORING AGENCY REPORT NUMBER

11. SUPPLEMENTARY NOTES

12a. DISTRIBUTION AVAILABILITY STATEMENT
APPROVE FOR PUBLIC RELEASE: DISTRIBUTION UNLIMITED.

12b. DISTRIBUTION CODE

13. ABSTRACT *(Maximum 200 words)*

A large part of the initial phase of this work involved the development and testing of the molecular dynamics computer code and associated analysis routines, to be used in the study of electrified jets and electrohydrodynamics of a number of common molecular and ionic fluids that are currently being used experimentally in these areas - along with fundamental interest in these systems, these studies aim at the application of electrified jets to colloid thruster technology. A major portion of our efforts was devoted to advance the computer algorithms to the point that we could simulate the operation of a colloid thruster and, as will be discussed below, we have entered this latter stage. Existing studies of electrified jets and electrohydrodynamic phenomena specifically involving the interaction of fluids with externally applied electric fields utilize continuum modeling and there have been no prior atomistic simulations in these areas. A significant component or our progress to date has been the development of parallel computer algorithms that can efficiently model systems as complex as a colloid thruster, yet be flexible enough to allow modeling of other interesting phenomena involving the electrodynamics of dielectric and charged fluids.

14. SUBJECT TERMS

20040520 052

15. NUMBER OF PAGES

16. PRICE CODE

17. SECURITY CLASSIFICATION OF REPORT	18. SECURITY CLASSIFICATION OF THIS PAGE	19. SECURITY CLASSIFICATION OF ABSTRACT	20. LIMITATION OF ABSTRACT

Nanojets: Electrification, Energetics, Dynamics, Stability and Breakup

Grant Number: F49620 – 01 – 1 -0426

Uzi Landman

School of Physics

Georgia Institute of Technology

Atlanta, Georgia 30332-0430

Final Report prepared for the

Air Force Office of Scientific Research

Period covered: June 1, 2001–November 30, 2003

I. Summary of Research Activities

This grant started on June 1, 2001, and in the following we report on research activities from that date to November 30, 2003.

Electrified Jets and Electrohydrodynamics of molecular fluids at the nanometer scale.

A large part of the initial phase of this work involved the development and testing of the molecular dynamics computer code and associated analysis routines, to be used in the study of electrified jets and electrohydrodynamics of a number of common molecular and ionic fluids that are currently being used experimentally in these areas – along with fundamental interest in these systems, these studies aim at the application of electrified jets to colloid thruster technology. A major portion of our efforts was devoted to advance the computer algorithms to the point that we could simulate the operation of a colloid thruster and, as will be discussed below, we have entered this latter stage.

Existing studies of electrified jets and electrohydrodynamic phenomena specifically involving the interaction of fluids with externally applied electric fields utilize continuum modeling and there have been no prior atomistic simulations in these areas. A significant component of our progress to date has been the development of parallel computer algorithms that can efficiently model systems as complex as a colloid thruster, yet be flexible enough to allow modeling of other interesting phenomena involving the electrodynamics of dielectric and charged fluids.

Since this project initiates a novel molecular-scale approach to the investigation of electrohydrodynamic phenomena, we have chosen to adopt a strategic staged approach, where we developed our research in stages of progressively increasing complexity. Our work falls roughly into two phases. The *first phase* encompasses the development of computer code of parallel architecture that uses well-tested atomic and molecular interaction potentials and most importantly the simulation code must compute in a very efficient manner the long-range Coulombic interactions between charged

species. The *second phase* involves building upon the simulation code described above so that one can model the complex geometries and electric fields present in a colloid thruster.

Phase One: Long-Range Interactions

As an early test of the developing computer code and as a guide in directing further work, we first studied single droplets of formamide with varying concentrations of sodium iodide in an external uniform electric field. This is a classic problem in the study of electrified fluids that has been studied both experimentally and theoretically and we expected that the comparison of our results to theoretical predictions would be very helpful. In fact, much of the important physics that is involved in colloid thrusters operating in the cone-jet mode is already present in the simpler problem of the elongation of a conducting liquid droplet in a uniform external electric field. The fluids that we currently focus on are the molecular fluid formamide along with ionic fluids, particularly sodium iodide which is one of the common ionic salts added to formamide to increase its conductivity and effectiveness in producing electrified jets in colloid thrusters.

In order to simulate systems that are sufficiently large to enable us to make contact with continuum behavior, the systems that we study could eventually contain hundreds of thousands of atoms and it is important to utilize simple efficient representations of the inter-atomic forces. Formamide is a planar molecule (see Fig.1) whose internal degrees of freedom and intra-molecular forces are of lesser significance for the phenomena in which we are interested here. Consequently, we treat the formamide molecule as a solid body using quaternion dynamics (ref. 1), implemented via a mid-step implicit leap-frog algorithm (ref. 2) that has been shown to be an extremely stable integration scheme (with only a very small energy drift occurring for long simulation periods). The geometry of the formamide molecule is taken from high-resolution X-ray studies of formamide crystals (ref. 3).

In our simulations we employed the AMBER force field parameters (refs. 4-5) for the intermolecular van der Waals interactions between the atomic sites located on different molecules, and also for interactions between the formamide molecule and the

ionic species (e.g. sodium iodide), as well as for the description of ion-ion interactions. For the atoms of the formamide molecule we use the CHELP-BOW (ref. 6) partial charges; these have been shown to give a good overall description of the electrostatic potential of the molecules. The weak inter-molecular van der Waals interactions are truncated on a group basis through the use of a smooth switching function (ref. 7) that depends on the distance between molecular centers of mass so that entire groups on one molecule interact with the entire group of atoms on another molecule, and dipole interactions are not truncated.

Our very first effort was to develop and test a computer code of parallel architecture for simulations of pure formamide and then we proceed to add the ionic components. As the computer code was developed we performed simple studies of liquid and solid formamide systems to test the code and to assess the ability of the interatomic potentials and the model that we use to reproduce basic known properties (such as solid and liquid densities and the melting point of formamide).

Since this is the first large-scale atomistic simulation involving electrohydrodynamics of complex fluids, we had to learn from our initial studies what features are essential in our computer code to faithfully model such systems. In particular, our initial code utilized long-range Coulombic interatomic potentials with finite interaction cutoffs as this was a simple first approach that is sufficient in many simulations. However when we ran test studies of pure formamide droplets in uniform external electric fields of varying strengths, we noted significant cooperative effects within the dipolar fluid that emerged as the cutoffs were increased from values of ~ 9 - 12 Å (typical values in many studies involving atomic partial charges) to 36 Å. Droplets (which when studied with small interaction cutoffs remain spherical) elongate as the cutoff is increased due to cooperative dipole-dipole and dipole-field interactions, in qualitative agreement with existing continuum theories of dielectric fluids in electric fields (ref. 12). From these observations it became apparent that the long-range interactions need to be treated much more accurately. The necessity of this became even more evident when our computer code was advanced to the point of allowing the addition of ionic salts to the dielectric fluid - their description especially requires a proper treatment of the long-range Coulomb forces. The development of our computer code to

address these issues is one of the most important parts of our progress and we will describe some of its capabilities in more detail, as well as discuss some of the issues that we have begun to study with it.

Fast multipole method (FMM). One of the most highly developed methods to efficiently model long-range forces is the *fast multipole method* (ref. 8), in which a system is spatially represented in a large (roughly) cubic "root-cell". The latter contains a hierarchy, or "tree-structure" division, of "child" sub-cells obtained by dividing the root-cell into octants and then allowing these child cells to be the parent cells of further binary subdivisions until one reaches the smallest "leaf" cell (see Fig.2). Multipole moments are computed for all cells at all levels from the atoms contained within the cells. Atoms in the basic leaf cell interact directly with all the atoms in neighboring leaf cells, while they interact with the multipole moments of more remote cells; the more remote the cells are from the central leaf cell, the larger they are allowed to be. Thus an atom interacts with a small set of multipoles representing entire, increasingly larger, volumes of remote space, rather than with all of the atoms contained within it - this is the main feature that makes it possible to efficiently model large systems involving long-range interactions.

Initially, we searched for existing FMM computer code that could be easily adapted for our needs as the FMM algorithm can be quite complex. While the basic FMM technique has been around for over a decade, its various forms and implementations are only beginning to evolve into standardized codes that can be simply adapted for general studies. We did not find an existing code that could be easily modified for the various types of systems and geometries of potential interest to us. Consequently, we further developed our computer code by formulating and programming our own parallel FMM algorithms. This affords us a lot of flexibility in our ability to modify and tailor our programs for different studies. Some of the features of our code are non-standard and many of the more standard features are not often found coexisting in one computer program.

Some of the main capabilities we have established in our code are:

1) The ability to replicate basic root-cells and "stack" them along a particular axis to create a long narrow tree-structure (requiring an appropriately modified non-standard

FMM algorithm). This is particularly useful for efficient simulations of systems such as highly elongated droplets and long liquid jets.

2) A large degree of flexibility in the choice of boundary conditions (bc's). We can employ periodic boundary conditions (pbc's) in one, two or three spatial directions, or perform "cluster simulations" where pbc's are not imposed at all. In simulations using pbc's in less then 3 directions, the non-periodic directions can be reflecting or absorbing. Absorbing bc's (any atoms that cross the system boundary are removed from the simulation) are necessary in simulations of fragmenting droplets or liquid jets where there are large fluxes of atoms crossing the finite boundaries (maintaining these atoms of the root-cell would cause artificial effects).

3) A modified FMM algorithm so that when using pbc's the tree-structure of the root-cell, along with all its computed multipoles, can be replicated any number of (specified) times as neighboring image cells. When this is done, atoms in the central computational cell see the correct multipole structure as they interact with neighboring periodic image cells out to any desired distance.

4) The ability to perform constant pressure simulations. The spatial dimensions of the root-cell can be allowed to vary, while using three-dimensional pbc's and the FMM, according to a modified constant-pressure algorithm due to Berendsen (ref. 1). This allows us to prepare bulk samples of both crystals and dielectric fluids with solvated ionic salts at any pressure or temperature of interest. These systems are useful for studying intrinsic bulk properties of materials currently being used in colloid thruster research. It also permits us to readily "carve out" droplets of various selected radii and charge for further more specialized studies.

As a simple check of both the computer code and the quality of the interatomic potential parameters, we performed a study that aims at finding the melting point of the simulated formamide for comparison with experimental data. Many experimental studies of liquid formamide are performed at room temperature, which is only about 25K above the experimental melting point of formamide. The potential parameters being used by us were not developed to specifically reproduce the melting point. Therefore, in anticipation of our simulations that involve formamide in the liquid state close to the melting point, it

is important to ascertain the thermodynamic properties of the simulated formamide. Our results from constant pressure simulations and liquid-solid coexistence studies indicate that that our description of formamide yields a liquid density that is in rather good agreement with experiments (to within a few percent) and a melting point that is approximately 10 degrees K above the experimental value of 275K.

Dielectric droplets in high electric fields

With the above in mind, we can now discuss the types of simulations being initiated using our parallel FMM code. First, we give some general information about the types of systems we explore and the materials involved. As mentioned earlier, these first simulations involve single droplets of formamide with varying concentrations of sodium iodide in an external uniform electric field. Dielectric and charged droplets in uniform electric fields are well-studied problems involving electrified fluids. Some of the most relevant physics involved in colloid thrusters operating in the cone-jet mode may be seen already in the simpler problem of an elongated conducting liquid droplet in a uniform external electric field, including the formation of electrified jets and emission and acceleration of small charged droplets at the ends of the elongated parent drops.

Our initial studies are performed at T=310K (see ref. 9) and involve droplets with a diameter of 10 nm. These droplets contain ~7150 formamide molecules (i.e. 6 x 7150 ~ 43000 atoms with partial charges). The droplets with added ionic salts have additional NaI molecules in two concentrations; in one the number of formamides to NaI molecules is 8:1 (~ 29 % NaI by weight, ~900 NaI molecules, i.e. 900 Na^+, 900 I^- ions solvated in the formamide fluid), and in the other the number of formamides to NaI molecules is 16:1 (~17 % NaI by wt, ~450 NaI molecules). The selection of these specific concentrations, as well as the choice of materials (formamide and NaI), were guided by current experiments on electrified jets and their role in colloid thrusters (refs. 10-11,13), in conjunction with the desire to allow comparisons with experimental findings.

It is noteworthy that the droplets simulated here are large enough to allow meaningful comparisons with continuum electrohydrodynamic theories, yet they are sufficiently small to enable us to perform (in a reasonably short time frame) a wide range of initial computer experiments. These studies should not only be relevant in order to

gain a better understanding of electrified jets – rather, they also allow a rapid development of analysis tools, methodologies and basic insights that will be important in the study of much larger systems.

In these early droplet simulations the basic root-cell of the FMM code has 8 tree levels with the smallest leaf cell chosen to be 1.2 nm on each side. This gives a root-cell of $2^{(8-1)}$ * 1.2 nm =153.6 nm dimensions on each side. This root-cell is replicated 3 times along the z-axis (the electric field direction) to give a total tree-structure of 153.6 nm x 153.6 nm x 460.8 nm in the center of which we place our 10 nm diameter droplet (see Fig.3). The very large system size allows enough room for the parent droplet to move and elongate freely and for secondary emissions to occur from any charged clusters leaving the parent drop. Absorbing bc's are used so that atoms reaching the system boundaries are removed. Once the simulation begins, no form of temperature control or control of the droplets center-of-mass motion is performed as we do not wish to risk introducing artificial effects.

Initially, we studied a pure formamide droplet, where a 10 nm diameter formamide droplet is placed in a constant uniform electric field along a given axis (the z-axis). The field strengths we use are on the order of 1 V/nm, a value that is of relevance to current research in these areas (ref. 11); this value of the field is large enough to generate a pronounced elongation of the formamide droplet. These simulations have begun and we plan to vary the field strengths over a wide range and compare the results using these nano-scale dielectric droplets to existing predictions of continuum theory (ref. 12). Our initial results indicate that in fields of ~1.0-1.5 V/nm these droplets will exhibit length/width aspect ratios on the order of ~15:1, (see Fig.1), roughly an order of magnitude smaller than the continuum predictions. Additionally we have discovered that the external electric field can induce crystallization of a droplet. Namely the external field modifies the thermodynamics and phase behavior of a dielectric droplet. While these studies are not our main focus, they also serve as interesting reference systems for our main study as they have no dissolved NaI but are otherwise similar to the formamide/NaI droplets.

In parallel with the simulations of pure formamide droplets described above, we have studied formamide droplets with dissolved salts. These droplets (10 nm in diameter)

had several concentrations of dissolved NaI and they were placed in constant uniform electric fields having strengths of 1.0-1.5 V/nm. Here we give a simple overview of this work and initial results. The behavior of these formamide/NaI droplets is significantly different than a pure formamide droplet. While the pure droplet elongates and reaches a steady state aspect ratio of ~15:1 with a relatively small degree of evaporation of formamide molecules, the salted droplet (29 % by wt NaI, field strength=1.5 V/nm) begins to deform (within ~10-20 ps after the application of the electric field) prior to the emission along the axial field direction, of positively and negatively charged clusters consisting of sodium and iodide ions solvated by formamide molecules. Over the course of about 1 ns, the parent droplet continues to elongate (to at most an ~8:1 aspect ratio) but it never achieves the long slender end points seen in the pure droplet due to the constant stream of ionic clusters of varying size breaking from its narrow end sections and being accelerated by the electric field (see Fig.4).

In Fig.5 we display (top to bottom) an early stage of the elongation process, detail of negatively charged fragments streaming off the droplet end during a later stage, and the system closer to the end of the simulation. Eventually, what remains of the parent drop fragments into two sizable clusters that in turn, as they are accelerated by the electric field, diminish in size as they emit a sizeable number of charged secondary clusters. When this salted droplet is placed in a lower field of 1.0 V/nm, the charged clusters that detach are larger. The smaller field elongates the droplet more slowly, giving more time for capillary forces to pinch off (the Rayleigh instability) larger sections of the droplet's slender end regions. We are beginning to observe and further explore phenomena that have not previously been studied at the atomistic level. We anticipated that the mechanisms of charged particle emissions from the slender ends of a droplet such as the one studied here, would be very similar in nature to those emerging from the extremely slender jet at the apex of a cone-jet in a colloid thruster – as we discuss below, we have indeed found such similarities.

In juxtaposition with the formulation and implementation of the simulation code, we have devoted significant efforts to the development of relevant methodologies for analysis of the "data" generated by the molecular dynamics simulations. As an example, one important program that we have developed allows us to go through the data of the

entire simulation and set virtual "detection planes" (see Fig.3) normal to the z-axis (electric field direction) at specified fixed distances above and below the parent drop, and record the statistics of all clusters that pass across the planes. Detailed information on these clusters is written to data files from which a variety of statistics can be quickly extracted. One also has the information saved so that any of the emitted clusters can be taken and allowed to continue evolving individually in a separate simulation.

To illustrate some of the more easily deducible statistics, we show in Fig.6 information derived from the simulation discussed above, i.e. a formamide droplet, containing 29 % (by weight) of dissolved NaI, placed in a uniform 1.5 V/nm external field. The detection planes were placed at ±200 nm along the z-axis (see Fig.3). The figure shows the abundances of overall flow statistics derived from the clusters passing these detector planes. In a simulation one is able to look in considerable detail at what contributes to the flow of material emanating from the ends of the elongated droplet. Fig.7(a) depicts the abundances of ion-containing clusters of different charge and shows that most of the observed clusters have charge ±1. A decomposition of this information is seen in Fig.7(b) that shows that in these abundant clusters (charge ±1) the largest contributions are from single ion clusters (Na^+ and I^- with adsorbed formamide molecules).

More detailed information is displayed in Fig.8(a) showing the number of singly charged clusters observed (i.e. positive Na^+, Na_2^+ I^-, etc. and negative I^-, Na^+ I_2^-, etc.) without regard to the number of accompanying adsorbed formamide molecules. While multi-ion clusters do contribute, the primary contribution is from single-ion clusters Na^+ and I^- and one sees that the ratio of Na^+ to I^- clusters is ~ 2:1. Fig.8(b) provides information related to the size and mass distribution of these single-ion clusters by showing the relative number of single-ion clusters having a specific number of adsorbed formamide molecules. The Na^+ clusters have predominantly 4-5 formamides while the I^- clusters exhibit a much broader distribution. It is interesting to note that experimental estimates (utilizing colloid thrusters and formamide/NaI mixtures) of the average number of adsorbed formamides lay within in this range of 4-5. This is also consistent with spectroscopic analysis (ref. 13) of $Na(FA)_n^+$ clusters (n is the number of formamide molecules $HCONH_2$, denoted here by FA). This experimental work employs a formamide

fluid with the same concentration of NaI as used in our simulations and instead of a droplet in an external field, it used a colloid thruster (at the mm length scale) to produce the charged clusters. The spectroscopic analysis indicates that for n > 4 the abundance of clusters falls off dramatically. This is of interest because if one estimates the energy necessary to remove one formamide molecule from $Na(FA)_n^+$ (see Fig.9, the energies displayed were obtained from simulations we performed of $Na(FA)_n^+$ at 300K for n=1-8) there is no abrupt change as n exceeds four. This is also consistent with other theoretical work (ref. 13) where the energies were derived from optimized $Na(FA)_n^+$ structures and quantum chemical calculations. Therefore, it is rather interesting and promising that results from our simulations, involving drops of FA/NaI mixtures at $\sim 10^2$ nm length scales and V/nm applied electric field strength, already begin to display similar phenomena and statistics as found in mm scale colloid thrusters where the field strengths due to the applied nozzle/extractor potentials can be considerably smaller.

We have found that if the detection planes are moved closer to the parent cluster, e.g. ± 100 nm, the formamide distribution (such as the one shown in Fig.8(b) for detection planes that are placed at ±200 nm) shifts very slightly to higher numbers. This leads us to conclude that the effects of molecular evaporation may be observed even relatively close to the emission source. This touches on an important point regarding these types of simulations and their relation to colloid thruster research. In laboratory experiments the charged clusters are studied far 'downstream' from the emitting source and the statistics of the clusters that are observed may be quite different than just after the clusters leave the emitting jet since a very large amount of evaporation, secondary emissions and fragmentation may take place. The mechanism of any thrust produced by the emitted charged species depends on its charge and mass starting at the instant of leaving the source, whether it is a Taylor-cone or parent droplet. Since these simulations allow us to study in great detail the nature of the charged species as they are actually being produced, we are in a unique position to provide useful insights on propellant properties and their role in thrust generation.

The work discussed above serves as a prelude to simulations of a colloid thruster where one wishes to understand in some detail the factors contributing to the thrust. The center-of-mass of the cluster in the simulation discussed above is stationary so that the

simulation may be regarded as mimicking two colloid thrusters back-to-back with opposite nozzle/extractor bias voltages. The thrust displayed in Fig.6 is the average of the two thrusts (their absolute values) due to charged clusters being pulled from the droplet and accelerated along the ± z-axis, parallel to the imposed field. Referring to Fig.10 we will discuss one example of the analysis tools that we have explored to better understand contributions to thrust from different types of charged clusters (the thrust calculations here are due to the positively charged clusters only). One way to define a per-cluster thrust contribution, T(i), is to define a local mass flow rate, associated with a cluster, e.g. the i-th cluster, to use in $T(i)=dm/dt \times u(i)$. The average of T(i) over all of the clusters gives an average thrust. Another way to estimate the overall thrust consists of evaluation of the quantity: (total average mass flow rate) × (avg. flow speed). Although the flow is highly non-uniform and composed of many cluster types, both approaches are found to yield the same order of magnitude.

Fig.10 displays the per-cluster contribution as a function of the total number of ions (positively and negatively charged) in the cluster. Note that clusters with a large number of ions and large mass have high individual thrust but there are relatively few of them so they don't contribute significantly to the average thrust, while clusters having few ions and contributing less (individually) to the total thrust are heavily weighted by their large numbers, and thus they comprise the largest thrust component. The idea is that individual cluster thrusts as well as energies, etc. can be correlated to a clusters mass, charge, number of ions, etc.

Phase Two: Complex Geometries and Electric Fields

While some of the issues pertaining to the properties of liquid droplets in electric fields will be pursued further, this work allowed us to proceed towards our primary goal –i.e., simulations of electrified nanojets and colloid thrusters. In the second phase of the project the computer code constructed for the purpose of simulations of droplets formed the basis for the development of a code that can model the complex geometry of a capillary needle and counter electrode (extractor plate) of a colloid thruster. In particular,

the electric field produced by an applied potential difference between the needle and plate is quite complex and this must be integrated into the parallel fast multipole method (FMM) code that was described earlier. There are also several additional components that are required. For example: (i) there has to be a means of replenishing the fluid atoms lost from the capillary as they exit and are accelerated by the external electric field; (ii) one has to be able to feed a fluid (in this case a dielectric fluid with dissolved salts) through the capillary needle either at a prescribed velocity or by means of a constant applied pressure; and (iii) an algorithm must be provided for neutralizing the charged ionic species that remain within the capillary as charge is transported away. In addition, we have made an effort to assure that the implementation of these elements would reflect, as closely as possible, the associated physical mechanisms present in an actual thruster.

The simulation is performed using the modified FMM code described earlier, where a basic cubic root-cell is duplicated along one axis (the z-axis) to create a region of space that is sufficiently large so that the design of the material elements and the required fields will fit within it; this is coupled of course to the requirement that the long-range forces of the charged species will be computed accurately. The focus is on colloid thrusters which typically involve a metallic capillary tube, or nozzle, possibly with a conical tip to focus the fields at it's tip, and a extractor plate, with a large hole, placed a certain distance away from the nozzle. The extractor plate is maintained at a chosen potential relative to the nozzle (see Fig.11).

Reservoir. To address the issue of a reservoir that will continually supply the nozzle with dynamic fluid atoms, we apply techniques that have been used in computer simulations of the formation, stability and breakup of nanojets (ref. 14), modified to perform with an ionic fluid (employing the FMM structure of our code), and designed to allow an effectively unlimited amount of reservoir material. A bulk fluid of the desired material (formamide with a prescribed concentration of NaI) is prepared at the desired working temperature (usually ~ 300K) and pressure. The first step is to take a cylindrical core of fluid (from the prepared bulk fluid) that will be placed and positioned inside the capillary tube. To do this, copies of the 3-D periodic calculation cell, used in the bulk fluid calculation, are placed together so that the width of the resulting block of fluid is larger than the desired nozzle inner diameter, and the length fills the nozzle. The fluid

atoms outside the desired radius are discarded (under the constraint of overall charge neutrality). In this way a relatively small bulk sample can be equilibrated and used to fill a nozzle. This fluid core still has a number of periodically replicated cells along the z-axis. A boundary is defined, acting effectively as a "piston", above which fluid atoms are treated dynamically and below which the reservoir fluid atoms are effectively frozen and the forces between these atoms need not be computed thereby saving a considerably amount of computational time (although forces between these atoms and the dynamic atoms are computed). The piston's z-axis position is exactly one leaf cell width (the smallest cell size of the FMM tree structure, see earlier discussion) above the bottom of the FMM root-cell – this is purposefully designed so that the dynamic atoms plus one layer of cells containing static reservoir atoms are within the root-cell (where forces can be computed), with the rest of the reservoir atoms being located outside the root-cell. This allows all of the dynamic atoms to interact with a portion of the static atoms.

The static reservoir atoms are moved (or pushed) forward into the lower end of the nozzle (the method of moving is discussed below). All of the atoms in the system fall into the categories of dynamic or static. As the static reservoir atoms cross the piston z-position they are treated fully dynamically. In the case of molecules, when a molecule's center-of-mass (cm) crosses the piston static/dynamic boundary the molecule's atoms are declared dynamic. Once an atom/molecule is declared as dynamic, it remains in this category for the duration of the simulation. For a prescribed distance above the piston (we use 3 nm), the newly dynamic fluid atoms are temperature controlled via stochastic thermalization. After this point the fluid atoms that are within a chosen distance of the nozzle walls are temperature controlled.

To discuss the method by which the reservoir material is replenished, recall that the cylindrical nozzle/reservoir material is comprised of several replications, n, of a periodic system with, e.g., a cell of width W_Z along the z-axis. Whenever an atom, or a molecule (i.e. the molecule's center-of-mass, cm), crosses the piston boundary and becomes dynamic, an exact copy of it is placed at the rear of the advancing "frozen" reservoir by subtracting nW_Z from the z-coordinate of the particle, and adjusting the result for the past advancements of the reservoir's cm. Using this method, one can construct the nozzle/reservoir fluid from a few replications of a relatively small unit cell

and reuse the reservoir material over and over. As mentioned, just beyond the piston, the fluid molecules are stochastically thermalized, erasing any effects of periodicity.

To move, or push, the reservoir material forward through the nozzle, we use one of two relatively simple methods. In the first, which we are currently using, the reservoir material is moved forward at a constant velocity. The second method corresponds to a constant pressure being applied to the reservoir fluid. The forces on the reservoir atoms with the dynamic atoms across the piston boundary are computed (divided by the piston's area, they give the time varying pressure on the piston and reservoir material). The desired constant externally applied pressure is multiplied by the piston area to produce its associated force. The difference between this force and the calculated force, along with the current cm velocity of the reservoir core, is then used in a simple integration algorithm to advance all of the reservoir material by a common amount at each time step.

Treating excess charges. In a colloid thruster, charged droplets are created and accelerated through the extractor plate resulting in charge imbalances and buildup in the thruster unit. So if the working fluid is formamide/NaI, then a negatively biased extractor plate will extract positively charged material (excess of Na^+) leaving an excess of I^- ions at the nozzle. It is currently believed that these ions lose their charge to the nozzle and form neutral molecules which are then lost through several processes, including: (i) evaporation, (ii) convective flow into the charged material leaving the system, (iii) diffusion either on the exterior the nozzle surface or back into the nozzles reservoir material. Namely, the general picture is that the excess charged ionic species left behind loses it's charge somewhere near the metallic nozzle and the resulting neutral species is effectively removed, without effecting the operation of the thruster. To model this mode of operation, and maintain a charge balance in the simulation of a colloid thruster, we have created the following algorithm. First a cylindrical test section is specified, having a narrow width along the z-axis that can be varied and having a radius that exceeds the expected base radius of the fluid before it tapers down due to the action of the externally applied field. The net charge from the atoms within the test volume is computed and when the charge becomes negative (for the case of excess I^- ions) the outermost I^- ion near the periphery of the test volume is removed from the system. Note that this does not

mean that the tapering form of the exit fluid, e.g. a Taylor cone, need be neutral. In fact, in a Taylor cone the surface has a charge density, and it is the interplay between capillary forces and the surface forces due to the external field that permits a steady state conical shape. Once a steady state is reached in the simulation, one expects that any excess charge beyond the surface charge will be neutralized near the nozzle and the above algorithm assures this by maintaining neutrality in a zone near the nozzle exit.

Boundaries. Before discussing the implementation of the external field we give a few details about the rules concerning the motion of atoms and the system boundaries. Boundaries of the system include the boundaries of the FMM root-cell (atoms that cross these are simply omitted from the system) as well as the metallic nozzle/plate material. The nozzle is created out of a solid block of a chosen metal by discarding the atoms outside the boundaries that define the nozzle. The extractor plate is created in a similar manner by using a defining boundary that is relatively thin, has a large circular hole, and is centered along the z-axis at the desired distance from the nozzle exit. The diameter of the hole is close to, and is smaller, than the width of a FMM root-cell, and the outer x-y boundaries of the extractor plate are outside of the FMM root-cell (The geometry and positioning of the nozzle and plate-electrode are further discussed in latter sections).

Particles can clearly not be allowed inside the nozzle/plate material and this is realized though the repulsive component of the particle-wall interactions. Namely, a primary function of the particle-wall forces is to keep atoms from crossing wall-boundaries, and these forces can vary from purely repulsive forces, modeling a non-wetting fluid, to a balance of attractive and repulsive forces (approximating known or desired interactions). These particle interactions with the walls (i.e. nozzle or extractor plate material) can be implemented in a number of ways. One method is to simply use appropriate atomic interaction potentials between all of the fluid material and all of the nozzle/plate atoms. This would necessitate a substantial increase in the required computational load. The basic operation of the simulated thruster is expected to be insensitive to certain details of these interactions and one can explore simpler representations of the particle-wall interactions that can be evaluated in a highly efficient

manner. With these considerations in mind, we describe below the manner in which we have implemented atom-wall interactions.

When charged (or neutral) material encounters the extractor plate outside of its hole radius, it may be expected to be neutralized (or remain neutral) and eventually migrate outside of the operational area of the thruster. As a first approximation of this circumstance, when any atom or molecule crosses the boundary defining the extractor plate, they are removed from the system. With regard to atom-nozzle interactions we note that the most important elements of the thruster operation are capillary forces and the interactions of the external field with the fluid atoms that have left the immediate vicinity of the nozzle exit. Thus, for example, if the assumed atom/nozzle forces lead to wetting of the exterior nozzle tip then the base of a Taylor cone will be anchored at the nozzle tip (as it should), and this wetting action can be achieved through forces that are a simple and efficient representation of more complex particle-wall forces. We have just entered in our simulations the stage of actual thruster operation and in line with the preceding discussion we initially take the nozzle walls to be smooth in the sense that interaction potentials are taken to depend only on the distance of the fluid atoms from the wall. For atoms close to a wall, we model the atom-wall interaction as a 3-9 Lennard-Jones (LJ) potential (that describes the interaction of an atom interacting with atoms comprising a half-space solid through a 6-12 LJ potential); the parameters of the interaction potential are chosen to be close to those of hydrocarbon-gold interactions (ref. 15). However, as discussed above, the actual values of the potential parameters are not expected to be of great importance, and they may be varied to achieve the appropriate wetting behavior.

Electric field. At this point, we will discuss one of the most important elements in the development of our simulation code, namely the addition of the electric field that depends on the nozzle and plate geometry and the potential difference between them. Once the nozzle/plate geometry, size, and placement have been chosen, we input them (along with the required potential difference) into a finite-element-method (FEM) program (see ref. 16) used to calculate the potential, $\Phi(z,r)$, and electric field, $\mathbf{E}(z,r)$, on a cylindrically symmetric 2-D grid that is large enough to encompass the entire

calculational cell (the root-cell). For example, in Fig.12 we show, with axial symmetry, the FEM boundaries (thick lines) that are positioned to lie near the surfaces of the nozzle and extractor plate. A higher density of nodes is used near the nozzle tip to obtain better resolution of the electric field.

The set of field values calculated at the nodes of the FEM mesh are mapped onto a cylindrical grid, and they are used as input to the colloid thruster MD simulation code. At any given time, the charged ions, or the molecular components having partial charges, have cylindrical coordinates lying within one of the grid cells on whose vertices the field values are known. Using the particle coordinates relative to the grid cell vertices one can then use a simple 2-D interpolation routine to compute, in cylindrical coordinates, the potentials $\Phi(z,r)$ and fields $\mathbf{E}(z,r)$ at the location of each of the charged particles. After resolving the electric field into its three components relative to the orthogonal Cartesian axes, the force on an atom, with charge q, is computed as $\mathbf{F}(r) = q\mathbf{E}(\mathbf{r})$ and potential energy $U(\mathbf{r}) = q\Phi(\mathbf{r})$ where $\mathbf{r} = (x,y,z)$.

Further details about the colloid thruster simulations, as well as observations concerning colloid thruster or electrospray operation at smaller length scales, can be discussed by reference to Fig.13, where we display a cross section of the FMM root-cell with areas that bound the metallic nozzle/extractor material shown as gray solid areas. It is within these areas that the FEM boundaries (Fig.12) are prescribed. The variation of the electric field strength is shown through the use of color gradations and the arrows point in the field direction. Equipotential lines are also shown. The extractor plate/nozzle potential difference is –50 V and because of the ~ 10^2 nm length scales, the field strengths reach values that are of the order of V/nm (see the Future Plans section for a discussion of these field strengths as compared to those encountered in devices defined on the mm length-scale).

Testing of the nano-thruster simulation code. Our present simulations, using the geometry and field values shown in Fig.13, have involved non-wetting walls. A sample of our results is shown in Figs. 14-16. We observe from Fig.14 (and a closer view provided in Fig.15), that the fluid cone emanating from the nozzle extends down to the piston; in this simulation the fluid is pulled by the applied electric field, as well as pushed

through the nozzle at a velocity of 6m/s. The speed of flow of the fluid jet in a 3 nm-wide region near the exit is 50 m/s. The flow accelerates towards the extraction plate, reaching velocities of 3000-5000m/s at and just past the plate (with the lower value corresponding to a formamide-solvated sodium iodide molecule, and the higher one corresponding to a solvated single sodium ion).

Other views of the simulated system are shown in Fig.16. This describes a nozzle whose wall material is unwetted by the fluid above a certain point, while below this point wetting occurs. In this study the two regions are of the same radius; however, we have the freedom to modify this configuration to one where the radius of the upper exit region is larger than that of the region to the left of the piston (see Fig. 15).

The material streaming from the leading edge of the exiting fluid consists of both evaporating neutral formamide molecules as well as positively charged clusters that are accelerated by the external fields through the extractor plate. Because of the high acceleration of detaching charged clusters, one generally observes only a few clusters between the end of the fluid cone and extractor plate. Once past the extractor plate, the charged clusters are in a much weaker field and they move essentially at a constant velocity. Note the similarities between the flow of the detaching charged clusters in Figs.14-16 for a colloid thruster and in Figs.4-5 for a droplet, in line with the expectation that both share a common physical description. The analysis programs used to calculate the statistics of emitted clusters from droplets in a constant electric field are being modified for use in the colloid thruster simulation. For example, a virtual 'detection plane' (Fig.3) may be placed at any desired distance from the nozzle exit and the statistics of the material crossing this plane collected and analyzed (the region of primary interest is just past the extractor plate).

Summary. To summarize this section, we remark that we have arrived at a stage where we have constructed, implemented and tested an efficient simulation code for investigations of the properties and mechanisms underlying the physical characteristics and operational principles of a colloid thruster. While some work still needs to be done to bring the simulation model closer to its experimental counterpart, the nontrivial task of constructing the most essential computer algorithms is completed.

Acknowledgements: We thank Rainer Dressler for helpful discussions and for sharing his work with us.

References:

1) M. P. Allen and D. J. Tildesley, *Computer Simulation of Liquids* (Clarendon, Oxford, 1987)

2) M. Svanberg, Mol. Phys. **92**, 1085 (1997).

3) E. D. Stevens, Acta Cryst. **B34,** 544 (1978).

4) W. D .Cornell, et al., J. Am. Chem. Soc. **117**, 5179 (1995).

5) www.amber.ucsf.edu/amber/ff94/parm.dat

6) E. Sigfridsson and U. Ryde, J. Comp. Chem. **19**, 377 (1998).

7) L. Perena, et al., J. Chem. Phys. **102**, 450 (1995).

8) L. F. Greengard, *The Rapid Evaluation of Potential Fields in Particle Systems* (The MIT Press, 1988).

9) The physics is not expected to be significantly different than for T=300K. Nevertheless, we work at a slightly higher temperature 310K to account for the 10°K higher melting point of the simulated formamide so that our results correspond more closely to 300K experimental results.

10) M. Gamero-Castano and V. Hruby, J. of Propulsion and Power **17,** 977 (2001).

11) M. Gamero-Castano and J. Fernandez de la Mora, J. Chem. Phys. **113**, 815 (2000).

12) H. A. Stone, J. R. Lister, and M. P. Brenner, Proc. R. Soc. London A **455,** 329 (1999).

13) Rainer Dressler, private communication. Also a presentation by Yu-Hui Chiu of his group at the Colloid Thruster / Nano Electrojet Workshop, Cambridge, MA, Oct. 3-4,2000.

14) M. Moseler and U. Landman, Science **289**, 1165 (2000).

15) T. K. Xia, J. Ouyang, M. W. Ribarsky and U. Landman, Phys. Rev. Lett. **289**, 69 (1992).

16) We use a readily available FEM code that may be freely downloaded at www.quickfield.com. This code is simple to use so that changes in the nozzle/extractor plate design and desired boundary conditions are relatively easy to implement.

17) J. Fernandez de la Mora, private communication.

18) J. Fernandez de la Mora and I. G. Loscertales, J. Fluid Mech. **260**, 155 (1994).

19) I. G. Loscertales, and J. Fernandez de la Mora, J. Chem. Phys. **103**, 5041 (1995).

FIGURES

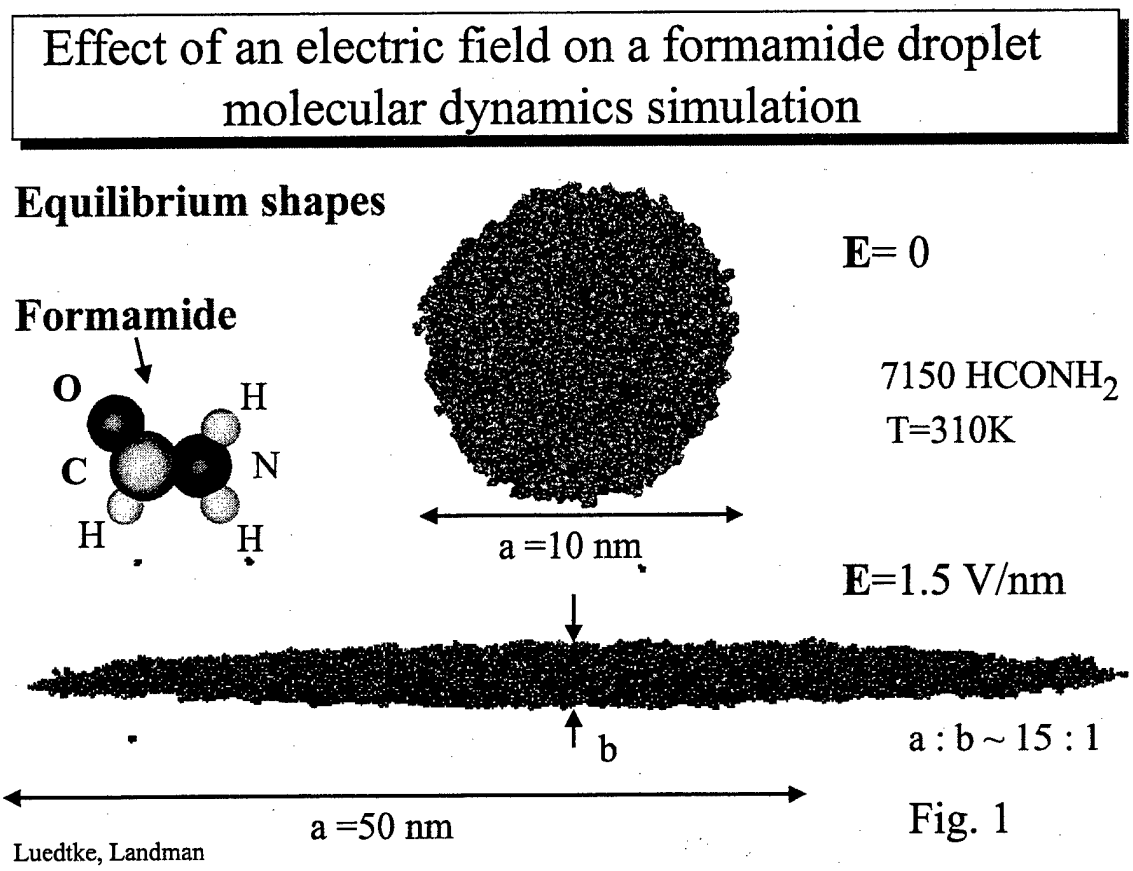

Fig. 1

Fast Multipole Method

- Binary Tree Structure Division of Space
- Atoms in adjacent cells interact directly
- Compute multipole moments of all cells at all levels from the atoms within the cells
- Atoms interact only with the multipoles of more distant cells

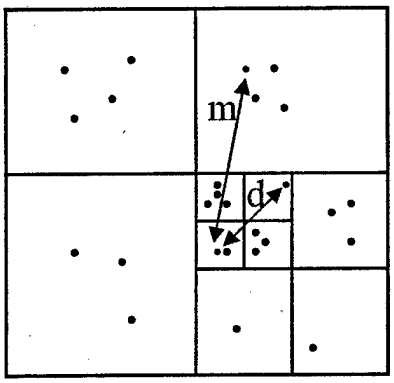

Fig 2

Luedtke, Landman

System Geometry

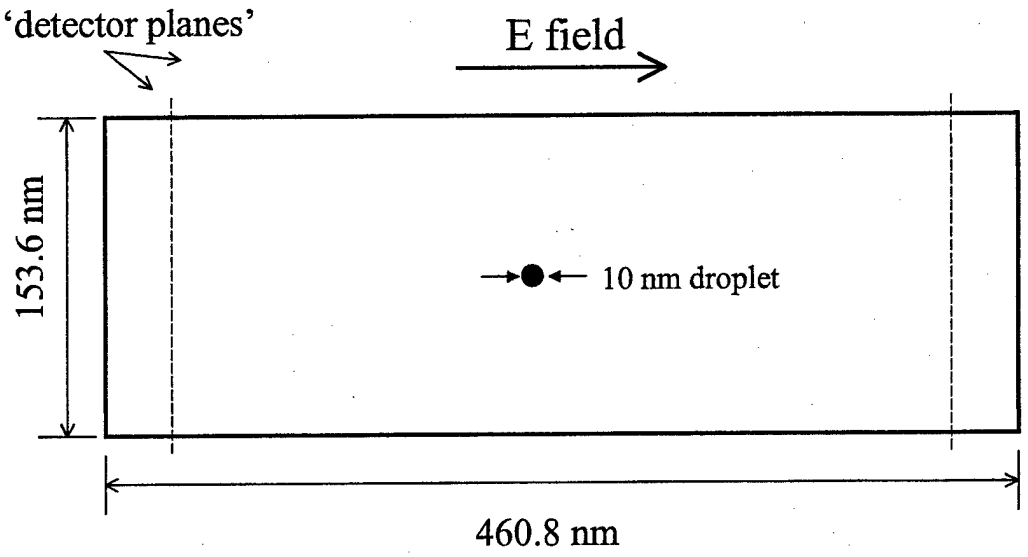

- 7150 Formamide molecules, 810 Na^+, 810 I^-

(detector planes normally set at $\pm$ 200 nm)

Fig 3

Luedtke, Landman

MD simulations of **electric-field-induced fragmentation** of a formamide / NaI droplet (29% NaI by weight)

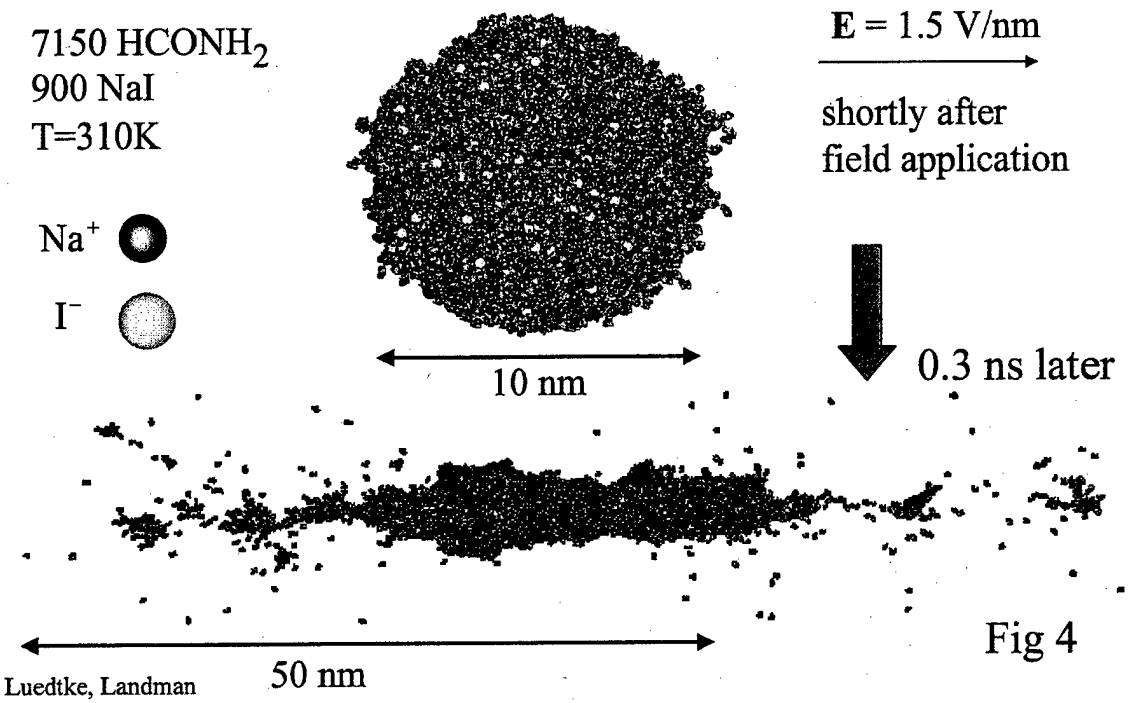

Luedtke, Landman

Fig 4

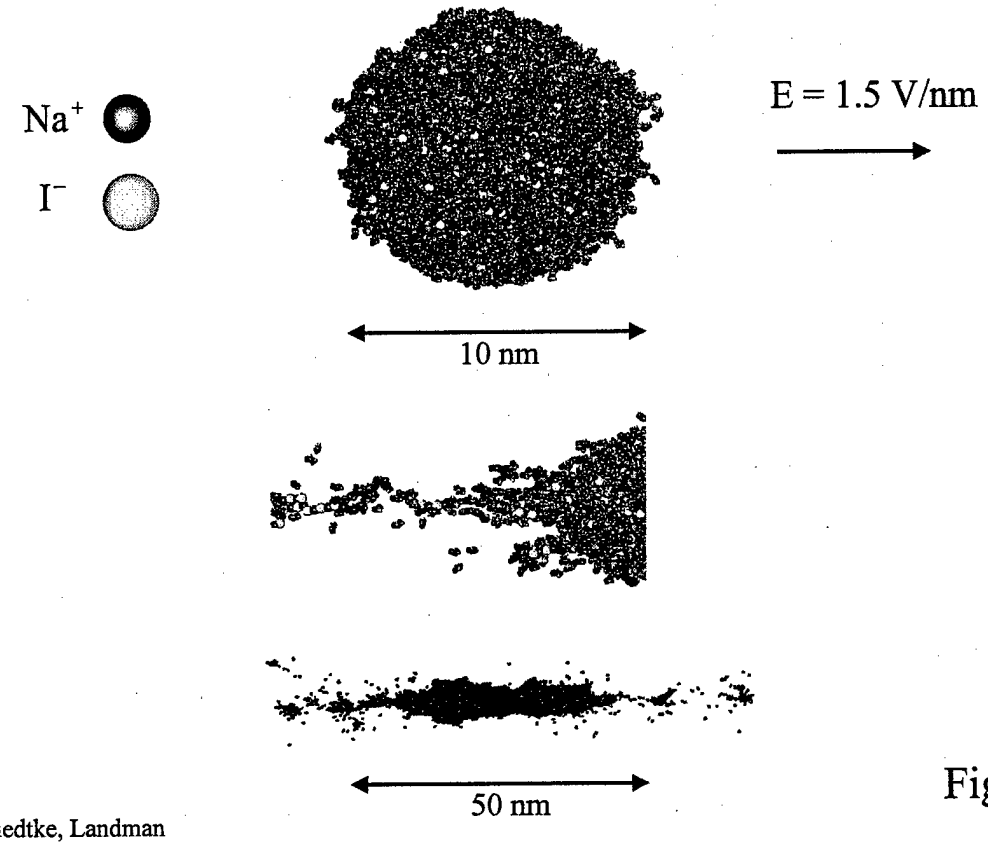

Fig 5

Luedtke, Landman

Cluster Flow Statistics

averaged over + and – flow E=1.5V/nm
Total flow rate ~ 4×10^{-4} nl/s
Charged flow rate ~ 2×10^{-4} nl/s
Current ~ 30 nA
Thrust~ 1.6 nN

Fig 6

Luedtke, Landman

Cluster Charge Statistics E=1.5 V/nm
(for clusters having an ionic component)

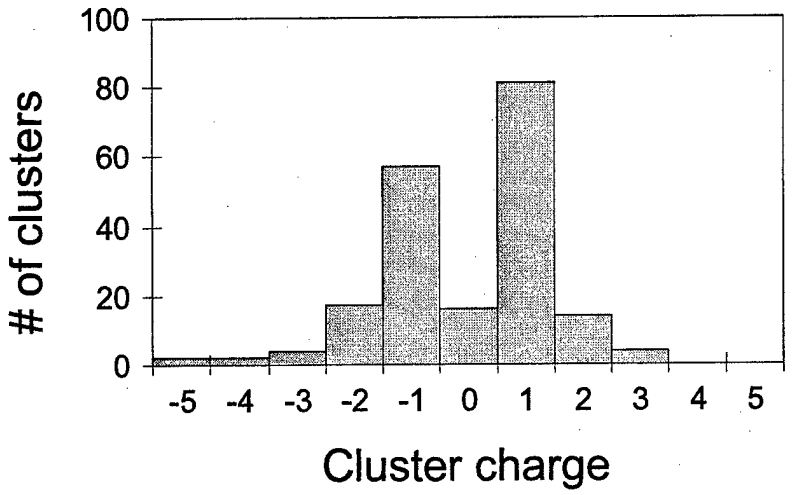

Fig 7 (a)

Luedtke, Landman

Cluster Charge Statistics E=1.5 V/nm

(for clusters having an ionic component)

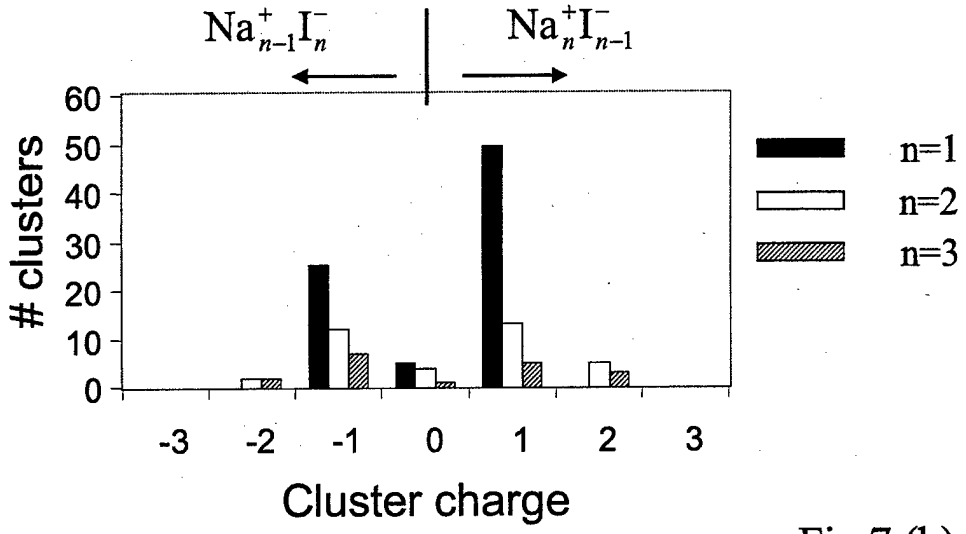

Fig 7 (b)

Luedtke, Landman

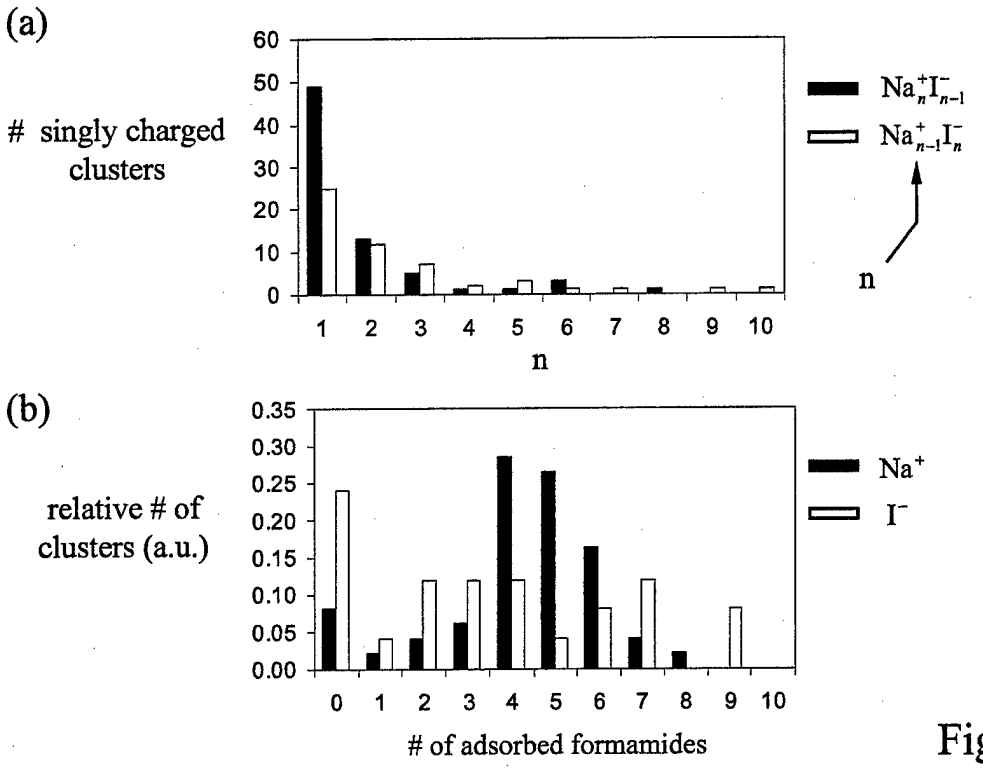

Fig 8

Luedtke, Landman

Formamide-Na^+ Energies (eV)

Energy per Formamide molecule in $Na^+(FA)_n$

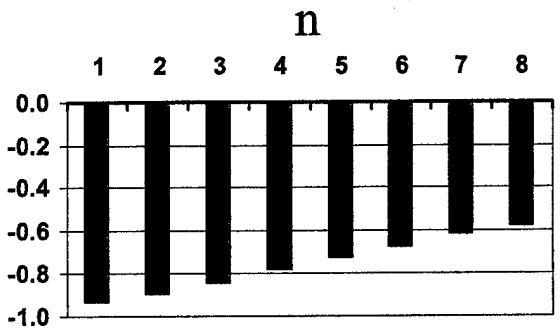

Energy to remove one Formamide from $Na^+(FA)_n$

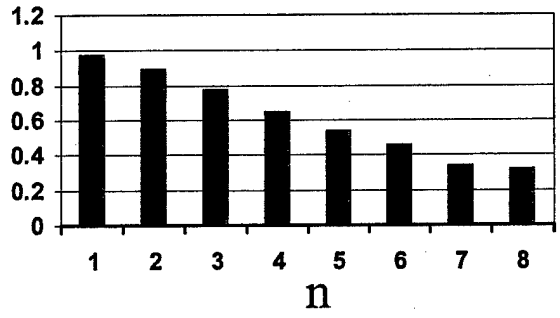

Fig. 9

Luedtke, Landman

Exploring ways of understanding results: *thrust contributions* T_i

t_i = time that cluster$_i$ passed detector plane

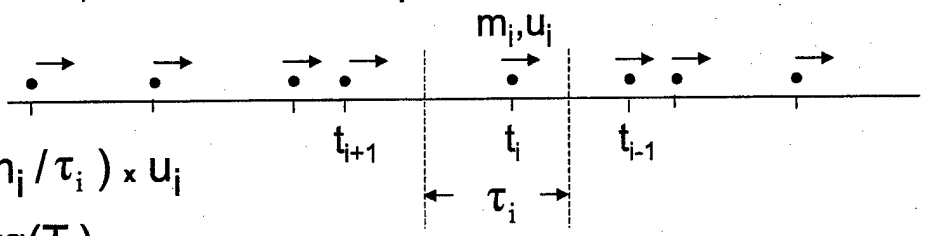

$T_i = (m_i / \tau_i) \times u_i$

$T = \text{avg}(T_i)$

~1.6 nN

Note: $\sum_i m_i / \sum_i \tau_i) \times \text{avg}(u_i) \sim 1.2\text{nN}$

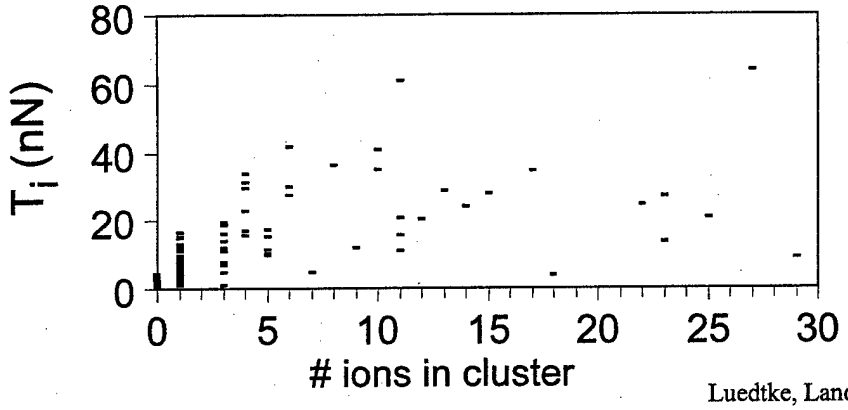

Luedtke, Landman

Fig. 10

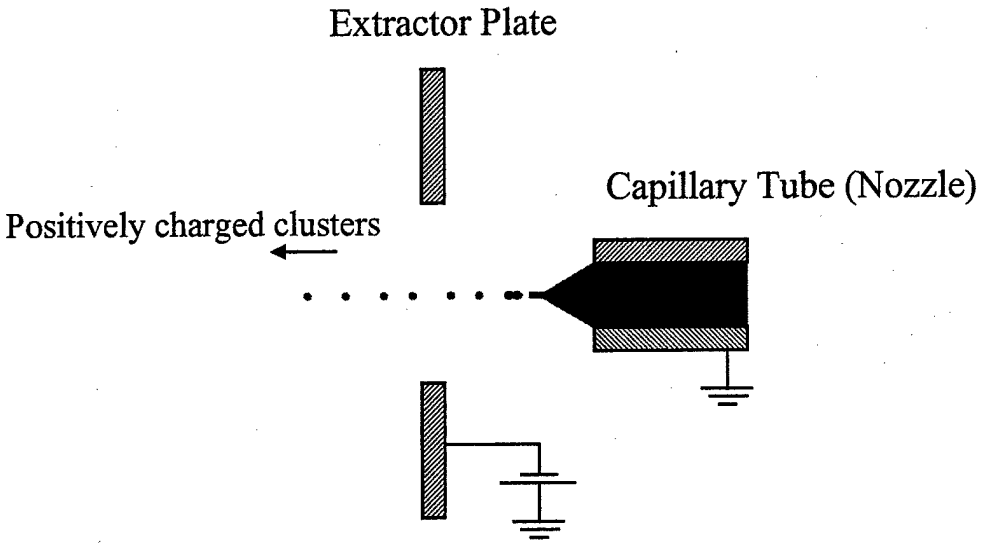

Fig. 11

Luedtke, Landman

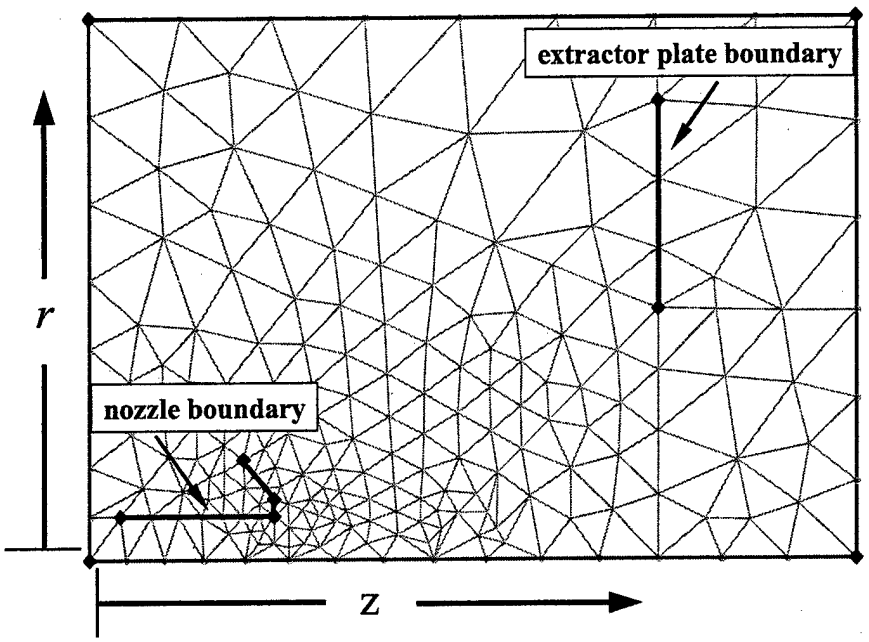

Fig. 12 Finite Element Geometry and Mesh

Luedtke, Landman

Colloid Thruster MD Simulation Geometry and Fields

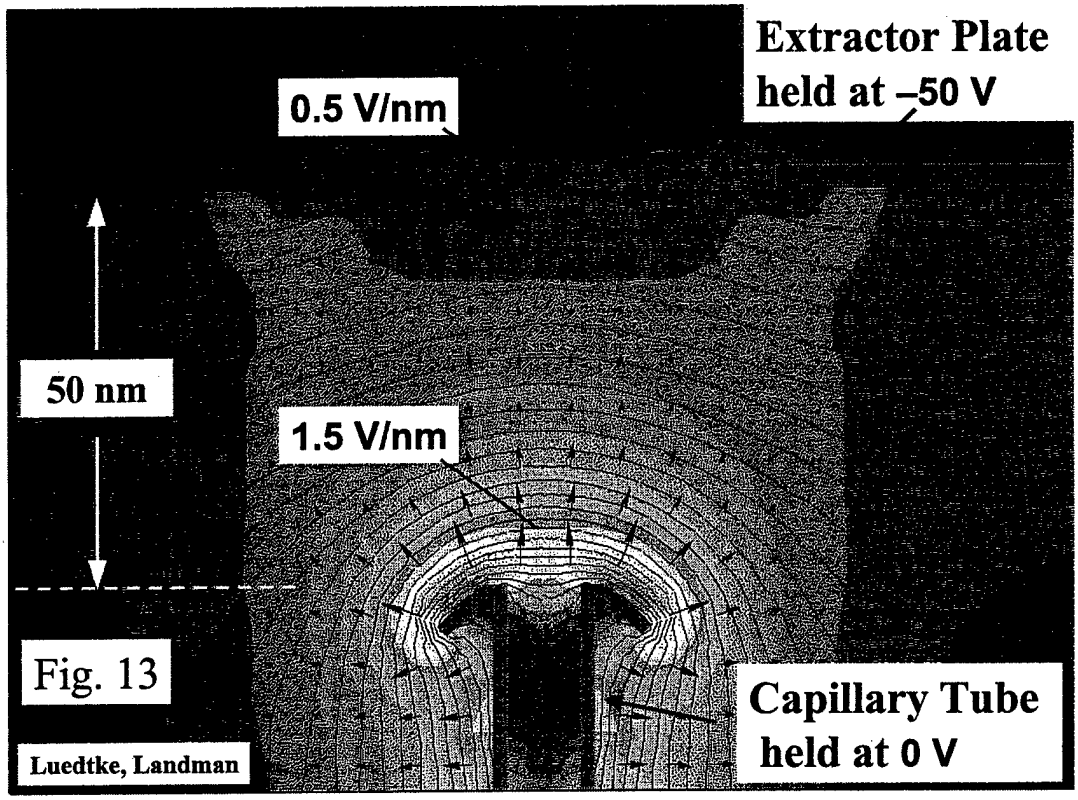

Fig. 13

Colloid Thruster with Non-wetting Walls

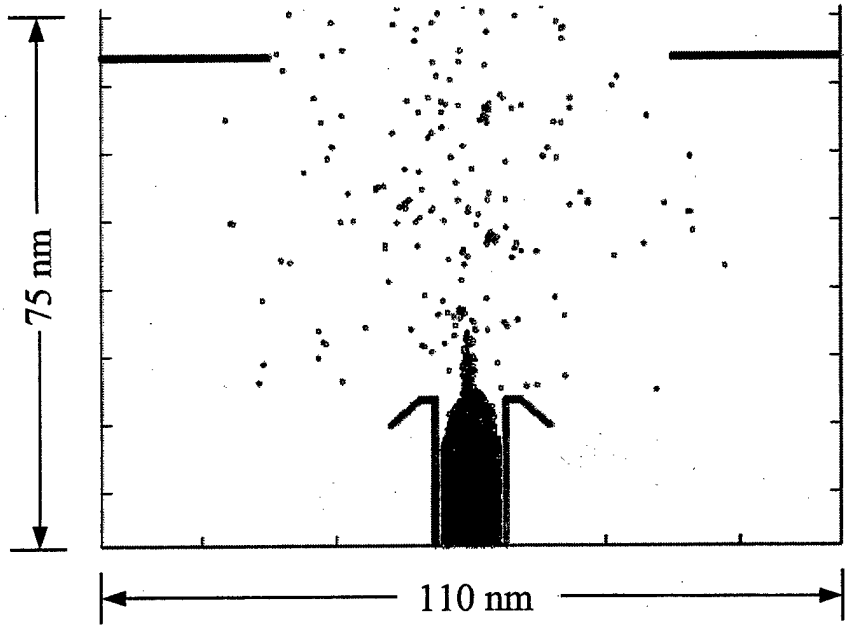

Fig. 14

Luedtke, Landman

Colloid Thruster with Non-wetting Walls

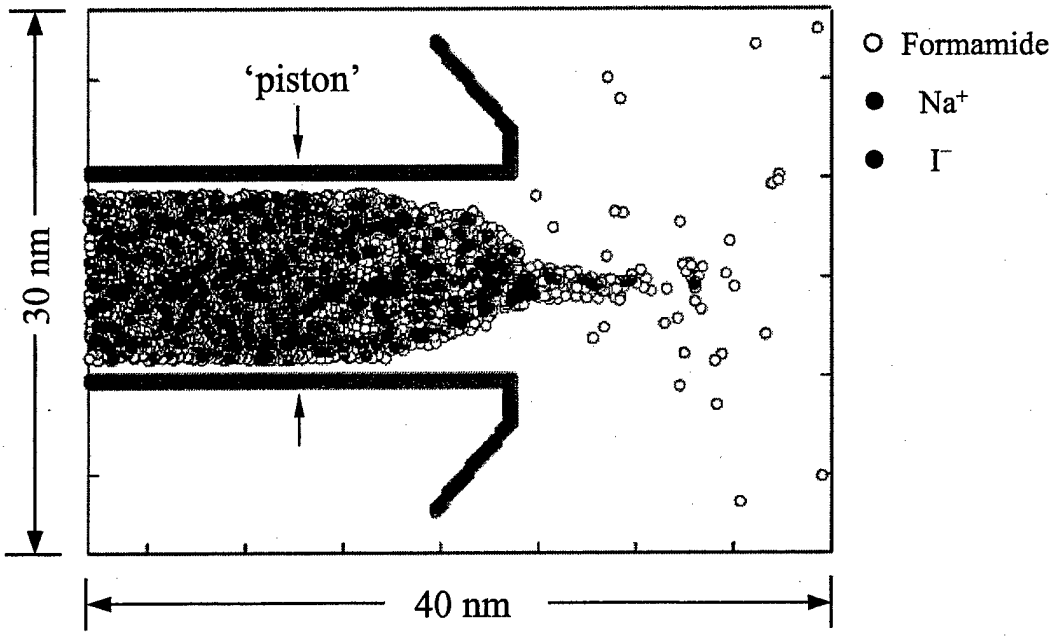

Fig. 15

Luedtke, Landman

Colloid Thruster MD Simulation

non-wetting walls, formamide/NaI (29% by wt)

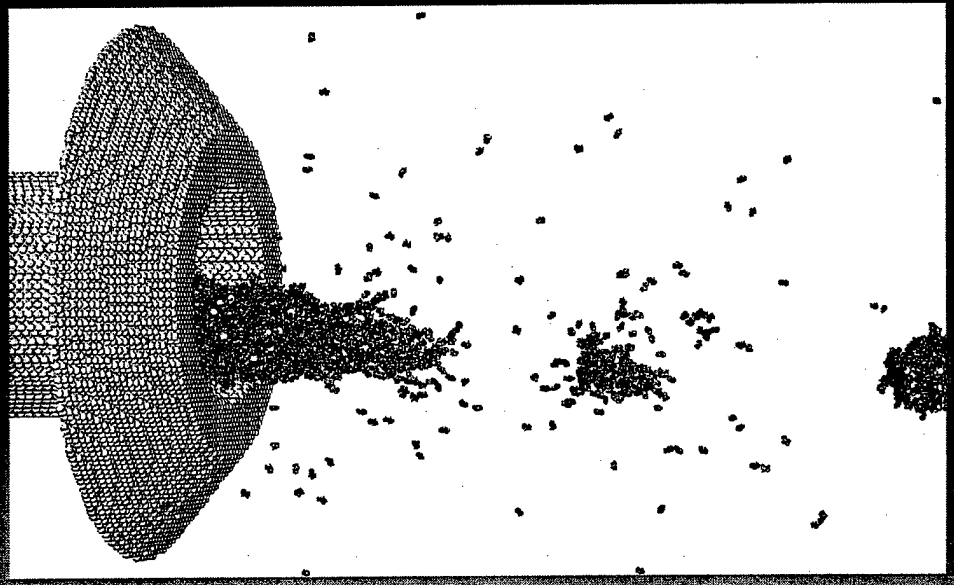

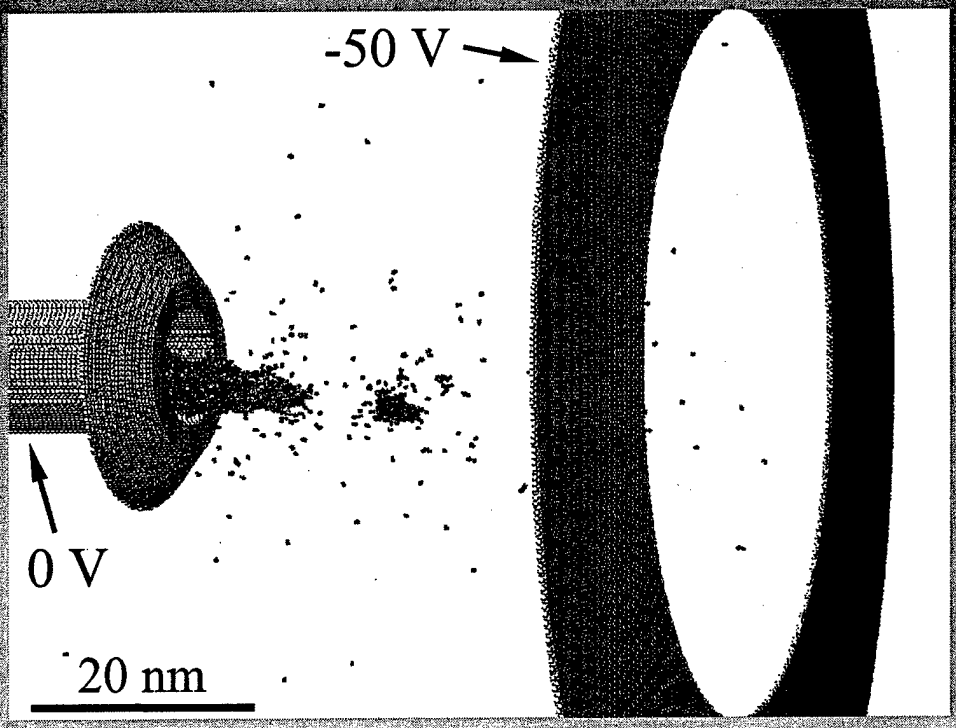

Luedtke, Landman

II. Major Accomplishments

Formulation, development, implementation and testing of efficient and flexible computational methodologies, algorithms and parallel computer codes for simulations and analysis of :

(a) Equilibrium and non-equilibrium properties of neutral or charged fluid droplets (consisting of up to tens of thousands of atoms), under field-free conditions and in the presence of applied electric fields.

(b) Generation, stability and breakup of fluid jets, driven by applied electric fields – modeling colloid thrusters of nanoscale dimensions.

The above simulation and analysis tools have been applied to investigations of geometrical and energetic properties of droplets and nanojets, made of a salt (NaI, 29% by weight) dissolved in formamide. (see section (I) of the report).

III. Interactions and Technology Transitions

In October 2002, Uzi Landman (PI) and W. David Luedtke presented the results of their studies in Boston at a workshop on electrified nanojets, organized by Dr. Rainer A. Dressler (Air Force Res. Laboratory, Space Vehicle Directorate, Hanscom AFB, MA).

IV. Supported Personnel

Dr. W.D. Luedtke, Senior Research Scientist – 100%

Dr. H. Hakkinen, Senior Research Scientist – 15%

Dr. C. L. Cleveland, Senior Research Scientist – 10%

Dr. J. Gao, Senior Research Scientist – 10%

V. Publications and Presentations

Several publications pertaining to methodological issues and description of the physical results of our simulations of dielectric dipolar droplets (with and without solvated ionic salts) in strong electric fields, are in the process of preparation.

Presentations:

The results of our investigations were reported at the March 2003 meeting of the APS (American Physical Society) in Austin, Texas, and the most recent results will be presented at the APS in Montreal (March, 2004)

Plenary Speaker (Landman), Nano-7/Ecoss-21, Malmo, Sweden, June, 2002.

Speaker (Landman), AFOSR Workshop on Electrified Nanojet and Colloidal Thrusters, MIT, Boston, October, 2002. Uzi Landman and David Luedtke (a Senior Research Scientist in Landman's group have participated in the workshop).

Invited Speaker (Landman), Conference on Cluster and Nanoscale Science, Nanjing University, Nanjing, China, March, 2003.

Keynote Speaker (Landman), Conference on Challenges in Computational Chemistry, Imperial College, London, England, April, 2003.

Invited Speaker (Landman), International Union of Vacum Societies Conference on NanoScience and Technology, Eilat, Israel, May 2003.

VI. Invention or Patent Disclosures

none

VII. Honors/Awards

The 2002 Medal of the MRS (Materials Research Society) ha been awarded to Uzi Landman.